REPORT

Bi-allelic variants in *SPATA5L1* lead to intellectual disability, spastic-dystonic cerebral palsy, epilepsy, and hearing loss

Elodie M. Richard,[1,76] Somayeh Bakhtiari,[2,3,76] Ashley P.L. Marsh,[2,3,76] Rauan Kaiyrzhanov,[4,76] Matias Wagner,[5,6,76] Sheetal Shetty,[2,3] Alex Pagnozzi,[7] Sandra M. Nordlie,[2,3] Brandon S. Guida,[2,3] Patricia Cornejo,[8,9,10] Helen Magee,[2,3] James Liu,[2,3] Bethany Y. Norton,[2,3] Richard I. Webster,[11] Lisa Worgan,[12] Hakon Hakonarson,[13] Jiankang Li,[14] Yiran Guo,[15,16] Mahim Jain,[17] Alyssa Blesson,[18] Lance H. Rodan,[19,20] Mary-Alice Abbott,[21] Anne Comi,[22,23] Julie S. Cohen,[22,23] Bader Alhaddad,[5] Thomas Meitinger,[5] Dominic Lenz,[24] Andreas Ziegler,[25] Urania Kotzaeridou,[25] Theresa Brunet,[5] Anna Chassevent,[22] Constance Smith-Hicks,[22,23] Joseph Ekstein,[26] Tzvi Weiden,[27] Andreas Hahn,[28] Nazira Zharkinbekova,[29] Peter Turnpenny,[30] Arianna Tucci,[31] Melissa Yelton,[32] Rita Horvath,[33] Serdal Gungor,[34] Semra Hiz,[35,36] Yavuz Oktay,[35,37] Hanns Lochmuller,[38] Marcella Zollino,[39,40] Manuela Morleo,[41] Giuseppe Marangi,[39,40] Vincenzo Nigro,[41,42] Annalaura Torella,[41,42] Michele Pinelli,[41] Simona Amenta,[39,40] Ralf A. Husain,[43] Benita Grossmann,[44] Marion Rapp,[45]

(Author list continued on next page)

Summary

Spermatogenesis-associated 5 like 1 (SPATA5L1) represents an orphan gene encoding a protein of unknown function. We report 28 bi-allelic variants in *SPATA5L1* associated with sensorineural hearing loss in 47 individuals from 28 (26 unrelated) families. In addition, 25/47 affected individuals (53%) presented with microcephaly, developmental delay/intellectual disability, cerebral palsy, and/or epilepsy. Modeling indicated damaging effect of variants on the protein, largely via destabilizing effects on protein domains. Brain imaging revealed diminished cerebral volume, thin corpus callosum, and periventricular leukomalacia, and quantitative volumetry demonstrated significantly diminished white matter volumes in several individuals. Immunofluorescent imaging in rat hippocampal neurons revealed localization of Spata5l1 in neuronal and glial cell nuclei and more prominent expression in neurons. In the rodent inner ear, Spata5l1 is expressed in the neurosensory hair cells and inner ear supporting cells. Transcriptomic analysis performed with fibroblasts from affected individuals was able to distinguish affected from controls by principal components. Analysis of differentially expressed genes and networks suggested a role for SPATA5L1 in cell surface adhesion receptor function, intracellular focal adhesions, and DNA replication and mitosis. Collectively, our results indicate that bi-allelic *SPATA5L1* variants lead to a human disease characterized by sensorineural hearing loss (SNHL) with or without a nonprogressive mixed neurodevelopmental phenotype.

Neurodevelopmental disorders (NDDs) frequently co-occur because disruption of early brain morphogenesis and connectivity can affect multiple intersecting domains of development. These disorders represent a wide spectrum of clinical manifestations, ranging from single organ (e.g., brain) pathology to embryonic lethality due to failure of

[1]Department of Otorhinolaryngology Head and Neck Surgery, School of Medicine, University of Maryland, Baltimore, MD 21201, USA; [2]Barrow Neurological Institute, Phoenix Children's Hospital, Phoenix, AZ 85016, USA; [3]Departments of Child Health, Neurology, Cellular, and Molecular Medicine and Program in Genetics, University of Arizona College of Medicine – Phoenix, Phoenix, AZ 85004, USA; [4]Department of Neuromuscular Disorders, Institute of Neurology, University College London, Queen Square, WC1N 3BG London, UK; [5]Institute of Human Genetics, Klinikum rechts der Isar, School of Medicine, Technical University of Munich, 81675 Munich, Germany; [6]Institute of Neurogenomics, Helmholtz Zentrum München, 85764 Neuherberg, Germany; [7]CSIRO Health and Biosecurity, The Australian e-Health Research Centre, Brisbane, QLD 4029, Australia; [8]Pediatric Neuroradiology Division, Pediatric Radiology, Barrow Neurological Institute, Phoenix Children's Hospital, Phoenix, AZ 85016, USA; [9]University of Arizona College of Medicine, Phoenix, AZ 85004, USA; [10]Mayo Clinic, Scottsdale, AZ 85259, USA; [11]Neurology Department, The Children's Hospital at Westmead, Westmead, NSW 2145, Australia; [12]Department of Medical Genomics, Royal Prince Alfred Hospital, Sydney, NSW 2050, Australia; [13]Center for Applied Genomics, Children's Hospital of Philadelphia, Philadelphia, PA, USA; [14]Department of Computer Science, City University of Hong Kong, Kowloon 999077, Hong Kong; [15]Center for Applied Genomics, Children's Hospital of Philadelphia, Philadelphia, PA 19104, USA; [16]Center for Data Driven Discovery in Biomedicine, Children's Hospital of Philadelphia, Philadelphia, PA 19146, USA; [17]Department of Bone and Osteogenesis Imperfecta, Kennedy Krieger Institute, Baltimore, MD 21205, USA; [18]Center for Autism and Related Disorders, Kennedy Krieger Institute, Baltimore, MD 21211, USA; [19]Division of Genetics and Genomics, Boston Children's Hospital, Boston, MA 02115, USA; [20]Department of Neurology, Boston Children's Hospital, Boston, MA 02115, USA; [21]University of Massachusetts Medical School – Baystate, Baystate Children's Hospital, Springfield, MA 01107, USA; [22]Department of Neurology and Developmental Medicine, Kennedy Krieger Institute, Baltimore, MD 21205, USA; [23]Department of Neurology, Johns Hopkins University School of Medicine, Baltimore, MD 21287, USA; [24]Centre of Child and Adolescent Medicine, Department of Pediatric Neurology and Metabolic Medicine, Heidelberg University Hospital, 69120 Heidelberg, Germany; [25]Department of Child Neurology and Metabolic Medicine, Center for Pediatric and Adolescent Medicine, University Hospital Heidelberg, Im Neuenheimer Feld 430, 69120 Heidelberg, Germany; [26]Dor Yeshorim, Committee for Prevention of Jewish Genetic Diseases, New York, NY 11211, USA;

(Affiliations continued on next page)

© 2021

Claudia Steen,[46] Iris Marquardt,[47] Mona Grimmel,[44] Ute Grasshoff,[44] G. Christoph Korenke,[47] Marta Owczarek-Lipska,[48,49] John Neidhardt,[48,50] Francesca Clementina Radio,[51] Cecilia Mancini,[51] Dianela Judith Claps Sepulveda,[51] Kirsty McWalter,[52] Amber Begtrup,[52] Amy Crunk,[52] Maria J. Guillen Sacoto,[52] Richard Person,[52] Rhonda E. Schnur,[52] Maria Margherita Mancardi,[53] Florian Kreuder,[54] Pasquale Striano,[55,56] Federico Zara,[56,57] Wendy K. Chung,[58] Warren A. Marks,[59,60] Clare L. van Eyk,[61,62] Dani L. Webber,[61,62] Mark A. Corbett,[61,62] Kelly Harper,[61,62] Jesia G. Berry,[61,62] Alastair H. MacLennan,[61,62] Jozef Gecz,[61,62,63] Marco Tartaglia,[51] Vincenzo Salpietro,[55,56] John Christodoulou,[64,65] Jan Kaslin,[54] Sergio Padilla-Lopez,[2,3] Kaya Bilguvar,[66,67] Alexander Munchau,[45] Zubair M. Ahmed,[1,68] Robert B. Hufnagel,[69] Michael C. Fahey,[70] Reza Maroofian,[4] Henry Houlden,[4] Heinrich Sticht,[71] Shrikant M. Mane,[66,67] Aboulfazl Rad,[72] Barbara Vona,[72] Sheng Chih Jin,[73] Tobias B. Haack,[44,74] Christine Makowski,[75] Yoel Hirsch,[26] Saima Riazuddin,[1,68,*] and Michael C. Kruer[2,3,*]

vital organs, yet common, recognizable NDD phenotypes include intellectual disability, hearing loss, cerebral palsy, autism, and epilepsy. Prior work has revealed that homozygous or compound heterozygous variants in the spermatogenesis-associated 5 gene (*SPATA5* [MIM: 613940]) cause an NDD syndrome[1] that features microcephaly, cortical visual impairment, intellectual disability, spastic cerebral palsy, epilepsy, and sensorineural hearing loss (SNHL) (MIM: 616577). Neuroimaging features included hypomyelination in some individuals and a thin corpus callosum. Based on the domain structure, SPATA5 has been grouped into the ATPase associated with diverse activities (AAA+) protein family.[2] Knockdown of *Spata5* in rat cortical neurons led to abnormal mitochondrial morphology and fission/fusion ratios,[3] suggesting a role in energy metabolism. In humans, SPATA5 has a paralog, spermatogenesis-associated 5 like 1 (SPATA5L1), that is 35% identical and 52% similar by *Drosophila* RNAi Research Center Integrative Ortholog Prediction Tool (DIOPT) alignment. Previous genome-wide association studies have found that *SPATA5L1* resides within a locus associated with chronic kidney disease in a combined North American and Dutch cohort,[4] which was replicated in Japanese[5] and Mongolian[6] cohorts. However, no Mendelian disease-associated variants have been previously reported in *SPATA5L1*.

[27]Dor Yeshorim, Committee for Prevention of Jewish Genetic Diseases, Jerusalem 9054020, Israel; [28]Department of Child Neurology, Justus-Liebig-University Giessen, 35392 Giessen, Germany; [29]Department of Neurology, South Kazakhstan Medical Academy, Shymkent 160001, Kazakhstan; [30]Clinical Genetics, Royal Devon & Exeter NHS Foundation Trust, EX1 2ED Exeter, UK; [31]Clinical Pharmacology, William Harvey Research Institute, Charterhouse Square, School of Medicine and Dentistry Queen Mary University of London, London EC1M 6BQ, UK; [32]Penn State Health Children's Hospital, Hershey, PA 17033, USA; [33]Department of Clinical Neurosciences, John Van Geest Cambridge Centre for Brain Repair, University of Cambridge School of Clinical Medicine, CB2 0PY Cambridge, UK; [34]Inonu University, Faculty of Medicine, Turgut Ozal Research Center, Department of Paediatric Neurology, 44280 Malatya, Turkey; [35]Izmir Biomedicine and Genome Center, Dokuz Eylul University Health Campus, 35340 Izmir, Turkey; [36]Department of Pediatric Neurology, Faculty of Medicine, Dokuz Eylul University, 35340 Izmir, Turkey; [37]Department of Medical Biology, Faculty of Medicine, Dokuz Eylul University, 35220 Izmir, Turkey; [38]Children's Hospital of Eastern Ontario Research Institute; Division of Neurology, Department of Medicine, The Ottawa Hospital, and Brain and Mind Research Institute, University of Ottawa, Ottawa, ON K1H 8L1, Canada; [39]Università Cattolica Sacro Cuore, Facoltà di Medicina e Chirurgia, Dipartimento Scienze della Vita e Sanità Pubblica, 00168 Roma, Italy; [40]Fondazione Policlinico A. Gemelli IRCCS, Sezione di Medicina Genomica, 00168 Roma, Italy; [41]Telethon Institute of Genetics and Medicine, 80078 Pozzuoli, Naples, Italy; [42]Department of Precision Medicine, University of Campania "Luigi Vanvitelli," 80138 Naples, Italy; [43]Department of Neuropediatrics, Jena University Hospital, 07747 Jena, Germany; [44]Institute of Medical Genetics and Applied Genomics, University of Tübingen, 72076 Tuebingen, Germany; [45]Institute of Systems Motor Science, University of Lübeck, 23538 Lübeck, Germany; [46]Department of Paediatric and Adolescent Medicine, St Joseph Hospital, 12101 Berlin, Germany; [47]University Children's Hospital Oldenburg, Department of Neuropaediatric and Metabolic Diseases, 26133 Oldenburg, Germany; [48]Human Genetics, Faculty of Medicine and Health Sciences, University of Oldenburg, 26129 Oldenburg, Germany; [49]Junior Research Group, Genetics of Childhood Brain Malformations, Faculty VI-School of Medicine and Health Sciences, University of Oldenburg, 26129 Oldenburg, Germany; [50]Research Center Neurosensory Science, University of Oldenburg, 26129 Oldenburg, Germany; [51]Genetics and Rare Diseases Research Division, Ospedale Pediatrico Bambino Gesù, IRCCS, 00146 Rome, Italy; [52]GeneDx, 207 Perry Parkway, Gaithersburg, MD 20877, USA; [53]Unit of Child Neuropsichiatry, Department of Clinical and Surgical Neurosciences and Rehabilitation, IRCCS Giannina Gaslini, Genoa 16147, Italy; [54]Australian Regenerative Medicine Institute, Monash University, Clayton, VIC 3168, Australia; [55]Pediatric Neurology and Muscular Diseases Unit, IRRCS Istituto Giannina Gaslini, 16148 Genoa, Italy; [56]Department of Neurosciences, Rehabilitation, Ophthalmology, Genetics, Maternal and Child Health, University of Genoa, 16142 Genoa, Italy; [57]Unit of Medical Genetics, IRRCS Istituto Giannina Gaslini, 16147 Genoa, Italy; [58]Departments of Pediatrics and Medicine, Columbia University, New York, NY 10032, USA; [59]Department of Neurology, Cook Children's Medical Center, Fort Worth, TX 76104, USA; [60]Department of Pediatrics, University of North Texas Health Science Center, Fort Worth, TX 76107, USA; [61]Robinson Research Institute, Faculty of Health and Medical Sciences, University of Adelaide, Adelaide, SA 5006, Australia; [62]Adelaide Medical School, Faculty of Health and Medical Sciences, University of Adelaide, Adelaide, SA 5000, Australia; [63]South Australian Health and Medical Research Institute, Adelaide, SA 5000, Australia; [64]Brain and Mitochondrial Research Group, Murdoch Children's Research Institute, Melbourne Department of Paediatrics, University of Melbourne, Melbourne, VIC 3052, Australia; [65]Discipline of Child and Adolescent Health, University of Sydney, Sydney, NSW 2006, Australia; [66]Yale Center for Genome Analysis, Yale University, New Haven, CT 06520, USA; [67]Department of Genetics, Yale University School of Medicine, New Haven, CT 06510, USA; [68]Department of Biochemistry and Molecular Biology, School of Medicine, University of Maryland, Baltimore, MD 21201, USA; [69]Ophthalmic Genetics and Visual Function Branch, National Eye Institute, National Institutes of Health, Bethesda, MD 20892, USA; [70]Department of Paediatrics, Monash University, Melbourne, VIC 3168, Australia; [71]Institute of Biochemistry, Friedrich-Alexander-Universität Erlangen-Nürnberg, 91054 Erlangen, Germany; [72]Department of Otolaryngology - Head and Neck Surgery, Tübingen Hearing Research Centre, Eberhard Karls University Tübingen, 72076 Tübingen, Germany; [73]Department of Genetics, Washington University School of Medicine, St. Louis, MO 63110, USA; [74]Centre for Rare Diseases, University of Tübingen, 72074 Tuebingen, Germany; [75]Department of Paediatrics, Adolescent Medicine and Neonatology, Munich Clinic, Schwabing Hospital and Technical University of Munich, School of Medicine, 80804 Munich, Germany
[76]These authors contributed equally
*Correspondence: sriazuddin@som.umaryland.edu (S.R.), kruerm@arizona.edu (M.C.K.)
https://doi.org/10.1016/j.ajhg.2021.08.003.

Here, as part of large-scale sequencing screens of individuals with SNHL and cerebral palsy, we detected bi-allelic, predicted deleterious variants in *SPATA5L1* (HGNC: 28762, GenBank: NM_024063.3). Using GeneMatcher[7] services, we subsequently connected with colleagues worldwide. Together, we report 28 unique *SPATA5L1* variants in 47 affected individuals from 28 (26 unrelated) families. All human subjects' studies were performed in accordance with the ethical standards of the responsible committee on human experimentation according to institutional and national standards. Proper informed consent was obtained for all participants. Sequencing was performed at numerous centers, but all used Illumina systems and institutional pipelines based on current GATK best practices.[8,9] Details regarding sequencing metrics and variant prioritization can be found in the supplemental material and methods. Among the identified variants, 25 were present in the cohort in compound heterozygous form and three were found as homozygous variants (Figure S1). Out of these three, one missense variant, c.1199C>T (p.Thr400Ile), also segregates in a compound heterozygous fashion in two other families. Most putatively damaging variants were private except for five that were detected in multiple families: c.527G>T (p.Gly176Val), c.1398T>G (p.Ile466Met), c.606_619dup14 (p.Glu207Glyfs*25), c.1199C>T (p.Thr400Ile), and c.2066G>T (p.Gly689Val); the former two were found in both the neurologic presentation and isolated hearing loss cases, and the latter two were found only in individuals with neurologic presentation. The pathogenicity of missense variants was predicted by ^{3} 3 algorithms (Table S1). None of the identified variants were found in homozygous form in gnomAD.

All affected individuals with bi-allelic variants in *SPATA5L1* presented with mild, moderate, or severe hearing loss, and about half (25/47, 53%) also exhibited neurologic features, particularly global developmental delay/intellectual disability (seen in all individuals with neurologic involvement). Other prominent neurological findings included spastic-dystonic cerebral palsy in approximately two-thirds, epilepsy (16/25, 64%), and cortical visual impairment (15/25, 60%). Clinical features of our cohort are summarized in Table 1 and Figure 1A (and detailed in Tables S2 and S3). Operational definitions for presence/absence of NDDs can be found in the supplemental material and methods. Case video review indicated visual impairment, impaired expressive language, intellectual disability, and mixed movement disorders with resultant orthopedic complications (Videos S1, S2, S3, S4, S5, and S6).

Most individuals exhibited a movement disorder, typically spasticity (17/25, 68%), dystonia (15/25, 60%), or a combination of these two forms of hypertonia (13/25, 52%). This usually occurred in a quadriplegic or generalized distribution. More than half (17/25, 68%) of the individuals had isolated hypotonia, although these individuals tended to be younger and may not have manifested their full motor phenotype. Some individuals were reported to exhibit ataxia, while non-epileptic myoclonus was identified in one. Stereotypies were seen in several individuals as well. The degree of cognitive impairment seen in affected individuals varied from severe to profound. For severely affected individuals, hyporesponsiveness to environmental stimuli was seen. Autistic features were absent except for in two individuals. Additional neuropsychiatric features were not reported, and behavior problems were not prominent. A combination of focal and generalized seizure types was reported. Few individuals (4/25, 16%) exhibited infantile spasms, often associated with a clinical diagnosis of West syndrome. Other forms of generalized seizures included myoclonic (7/25, 28%), absence (3/25, 12%), and generalized tonic-clonic (11/25, 44%) events. Focal epilepsy (4/25, 16%), sometimes with secondary generalization, was evident in several individuals as well, and a subset demonstrated mixed focal and generalized semiologies. One individual was reported to have evidence of electrical status epilepticus in slow wave sleep (ESES), and seizures in some were intractable or described in the context of a developmental or epileptic encephalopathy.

Microcephaly was present in about half of the affected individuals (13/25, 52%). Facial dysmorphism, assessed locally and confirmed by a trained dysmorphologist (M.C.F.) whenever possible, was noted in one-third (9/25) of affected individuals. Facial features included downslanting palpebral fissures, widow's peak, low frontal hairline, large ears, tooth malformation, high palate, bitemporal narrowing, sparse eyebrows, depressed nasal bridge, and micrognathia as well as prominent upper lip, small chin, and mild telecanthus, evident in individual facial photographs (Figure 1B). A gestalt representation of "SPATA5L1 facies" was also constructed with the Face2Gene RESEARCH application (FDNA, Boston, MA, USA). However, this facial gestalt did not highlight any consistent dysmorphism, evidenced by the lack of a significant difference between the case and the age-, sex-, and ethnicity-matched control cohort ($p = 0.223$, Figure S2).

Neuroimaging findings were assessed by a board-certified neuroradiologist (P.C.). Some individuals' brains were morphologically normal, but relatively consistent features included diminished cortical volume, periventricular leukomalacia, widened Sylvian fissures, anterior temporal hypoplasia, and hypoplastic corpus callosum (Figure 2A). More variable features included delayed myelination in toddlers, an "ears of the lynx"-like appearance, incomplete hippocampal rotation, optic nerve hypoplasia, and small pons. To further characterize the structural neuroanatomic findings, we performed a quantitative volumetric analysis with DICOM data from clinical magnetic resonance images by using a previously described method.[10] This analysis revealed a significance decrease in white matter volume in *SPATA5L1* cases compared to controls (Figure 2B).

Intriguingly, a subset of individuals (DY1–DY11) with bi-allelic *SPATA5L1* variants presented with isolated, non-syndromic hearing loss without neurological features (22/47, 47%, Figure S1, Table S2). These individuals were all of Ashkenazi Jewish decent, and in all, the missense variant

Table 1. Bi-allelic variants in *SPATA5L1* cause a neurodevelopmental disorder featuring intellectual disability, cerebral palsy, epilepsy, and hearing loss

Family	Family 1	Family 2	Family 3	Family 4	Family 5	Family 6	Family 7	Family 8	Family 9
Patient	1 (proband)	3 (proband)	5	6	7	8	9	10 (proband)	13
cDNA (GenBank: NM_024063.3)	c.1304_1305del (pat.); c.121G>C (mat.)	c.734T > A (pat.); c.1398T>G (mat.)	c.1A>T (pat.); c.2066G>T (mat.)	c.515C>A (pat.); c.196G>T (mat.)	c.1973G>A (pat.); c.2176_2177del (mat.)	c.76A>G (pat.); c.1079T>C (mat.)	c.1556C>A (hom.)	c.1199C>T (hom.)	c.1676delC (pat.); c.1682T>C (mat.)
Protein (GenBank: NP_076968.2)	p.Ile435Argfs*4 (pat.); p.Ala41Pro (mat.)	p.Val245Glu (pat.); p.Ile466Met (mat.)	p.Met1? (pat.); p.Gly689Val (mat.)	p.Pro172His (pat.); p.Asp66Tyr (mat.)	p.Arg658Lys (pat.); p.Val726Lysfs*13 (mat.)	p.Thr26Ala (pat.); p.Phe360Ser (mat.)	p.Ala519Asp (hom.)	p.Thr400Ile (hom.)	p.Ala559Glufs*33 (pat.); p.Leu561Ser (mat.)
Ancestry	Iraqi	European, with Ashkenazi Jewish ancestry	American; mat. ethnicity, Italian; pat. ethnicity, Italian and Afro-American	mixed European	Spanish	African American	Turkish	Kazakh	mixed, Eastern European, and Scandinavian
Sex	male	male	female	male	male	female	female	female	male
Age at diagnosis	first year of life	32 months	27 months	23 years	4 months	9–12 months	5 years	7 months	1 month
Hearing impairment	+	+	+	+	+	+	+	+	+
Spasticity	+	−	+	−	−	−	+	+	+
Dystonia / hypotonia	+ / −	+ / +	− / +	− / N/A	− / +	N/A / −	+ / −	+ / +	− / +
Pattern	spastic quadriplegia	N/A	spastic quadriplegia	N/A	N/A	N/A	spastic-dystonic tetraparesis	spastic quadriplegia	spastic quadriplegia
Microcephaly (HC)	+ (acq., 47 cm at 6 years)	−	+ (acq., 46 cm at 3 years)	−	+ (acq., 45 cm at 1 year)	−	+ (27 cm at birth)	+ (45 cm at 6 years)	−
DD / ID	+ profound DD	+ global DD	+ global DD	+ severe DD	+ profound DD	+	+ severe DD	+ profound DD / ID	+ profound DD
Epilepsy	+	−	−	+	−	+	+	+	+
Dysmorphic features	−	+	−	−	−	−	−	+	+
Visual impairment	cortical visual blindness	−	cortical visual impairment	−	−	N/A	severe cortical visual impairment	probable cortical blindness	severe impairment
MRI findings	progressive CO and CB volume loss; thin CC; periventricular T2 hyperintensities; subtle GP hyperintensity bilaterally	concern for delayed myelination	delayed myelination; thin CC	CC lipoma, otherwise normal	normal	thin CC; enlarged 4th ventricle; mega cisterna magna; possible brainstem hypoplasia; possible delayed myelination	profound cortical atrophy with predominant reduction of the white matter; cerebellum and brainstem normal	paucity of periventricular WM bilaterally with patchy confluent T2 hyperintensity; thin CC; generalized CO atrophy	normal (age 14 months); repeat MRI showed diminished cortical volume

Family	Family 10	Family 11	Family 12	Family 13	Family 14	Family 15	Family 16	Family 17	Family 18
Patient	14	15	16 (proband)	18	19	20	21	22 (proband)	25

(*Continued on next page*)

Table 1. ***Continued***

Family	Family 10	Family 11	Family 12	Family 13	Family 14	Family 15	Family 16	Family 17	Family 18
cDNA (GenBank: NM_024063.3)	c.190C>T; c.1826C>G	c.85T>G (hom.)	c.1199C>T (pat.); c.1090−2A>G (mat.)	c.2066G>T (pat.); c.527G>T (mat.)	c.527G>T (pat.); c.2006T>G (mat.)	c.527G>T; c.1199C>T	c.213T>G; c.1313T>C (hom.)	c.1091T>A (pat.); c.1918C>T (mat.)	c.1648_1649insC; c.2066G>T
Protein (GenBank: NP_076968.2)	p.Arg64Trp; p.Ser609*	p.Cys29Gly (hom.)	p.Thr400Ile (pat.); p.? (mat.)	p.Gly689Val (pat.); p.Gly176Val (mat.)	p.Gly176Val (pat.); p.Met669Arg (mat.)	p.Gly176Val; p.Thr400Ile	p.Phe71Leu (hom.); p.Leu438Pro (hom.)	p.Val364Glu (pat.); p.Arg640* (mat.)	p.Phe550Serfs*16; p.Gly689Val
Ancestry	African American	Turkish	European (German)	Italian	European (German)	German	Arabian	German	Italian
Sex	male	male	male	male	female	male	male	male	male
Age at diagnosis	3 months	14 months	5 years	5 years, 6 months	2–3 months	15 years, 6 months	8 weeks	14 years, 9 months	5 months
Hearing impairment	+	+	+	+	+	+	+	+	+
Spasticity	+	−	+	+	+	+	+	+	+
Dystonia / hypotonia	+ / +	+ / −	+ / +	+ / +	+ / +	+ / +	+ / +	+ / +	+ / +
Pattern	spastic quadriplegia	quadriparesis	spastic quadriplegia	spastic quadriplegia	spastic quadriplegia	hypotonic dystonic spastic quadriplegia	hypotonic dystonic spastic quadriplegia	hypotonic dystonic spastic quadriplegia	hypotonic dystonic spastic quadriplegia
Microcephaly (HC)	+	+ (34 cm at birth)	−	+ (acq.)	+ (cong.)	+ (−2 SD at 1 year)	+ (32 cm at birth)	−	+ (48 cm at 6 years)
DD / ID	+ profound global DD	+	+ profound global DD	+ severe ID	+ severe ID	+ profound global DD	+ profound global DD	+ profound global DD	+ profound global DD
Epilepsy	+	+	−	+	−	+	+	+	+
Dysmorphic features	−	−	−	+	−	N/A	+	−	+
Visual impairment	−	−	mild myopia	N/A	severe impairment	−	severe impairment	severe impairment	central visual impairment
MRI findings	diffusely diminished CO volumes; ex vacuo dilatation LV; delayed myelination; thin CC	bilateral peritrigonal hyperintensity	diminished CO volume; periventricular WM hyperintensity	ventricle enlargement (slight); WM hyperintensity	diffuse slightly diminished CO volume; thin CC; lactate peak visualized on MRS (2 years)	mildly diminished CO volume; mildly atrophic BG; delayed myelination of the CC	mega cisterna magna; embryonic variant posterior cerebral artery	normal (11 months); slightly enlarged ventricles (19 months); no progression of ventricular enlargement (25 months); delayed myelination, thin CC (4.5 years)	brain hypomyelination; diffuse slight brain atrophy

Abbreviations: CO, cortical; CB, cerebellar; CC, corpus callosum; DD, developmental delay; ID, intellectual disability; GP, globus pallidus; WM, white matter; BG, basal ganglia; MRS, magnetic resonance spectroscopy; mat., maternal; pat., paternal; hom., homozygous; +, clinical feature detected; −, clinical feature not observed; N/A, no information provided for clinical feature; SD, standard deviation; p, percentile; acq., acquired postnatally; cong., congenital; HC, head circumference. T2 is an MRI signal acquisition parameter.

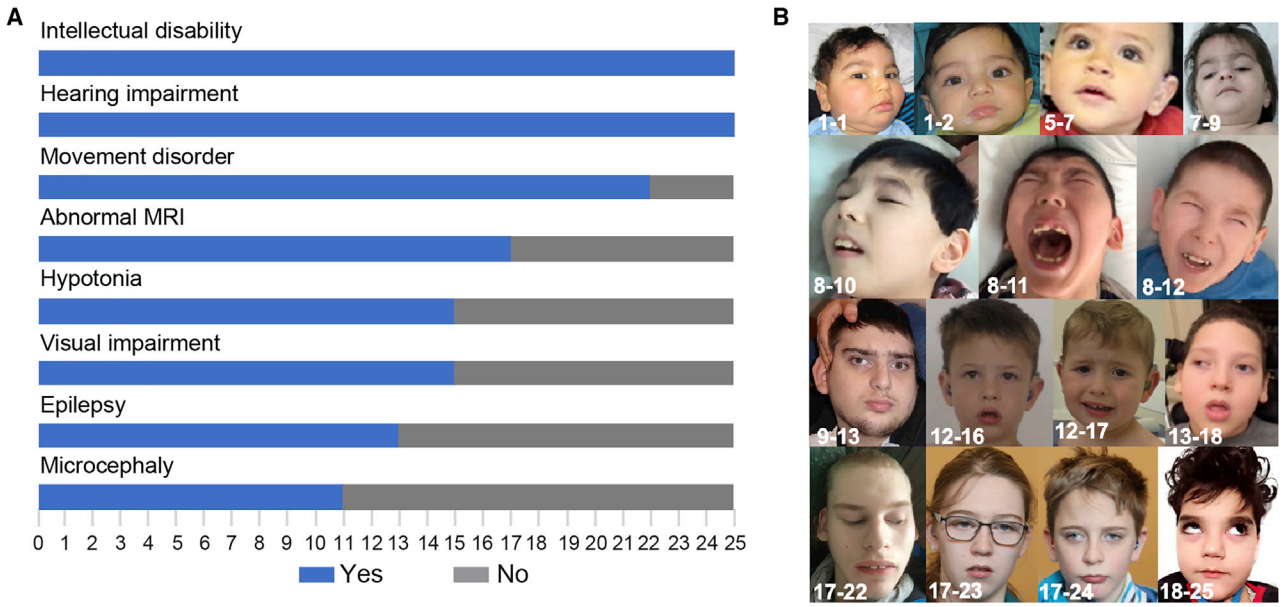

Figure 1. Prevalent clinical features of individuals with bi-allelic variants in *SPATA5L1*

(A) Bar graph illustrating the prevalence of the most relevant clinical features from the 25 individuals for whom full datasets were available from 18 families with the neurodevelopmental phenotype. Blue: individuals with the clinical feature. Gray: individuals without the clinical feature.

(B) Representative clinical features of individuals carrying bi-allelic *SPATA5L1* variants with the severe neurodevelopmental phenotype, showing subtle and non-specific dysmorphic features, including downslanting palpebral fissures, bitemporal narrowing, and depressed nasal bridge.

c.1398T>G was identified in compound heterozygosity with various other pathogenic alleles, suggesting a hypomorphic founder allele, resulting in a partial rather than complete loss-of-protein function. According to gnomAD, the allele frequency of this variant is 0.0029 in individuals of Ashkenazi Jewish background, indicating a frequency of homozygotes of 0.8/100,000. The fact that no individuals with SNHL hearing loss and homozygosity for the c.1398T>G allele were identified further raises the question whether the variant would not lead to a clinical phenotype in homozygous form. Like the cases with neurologic involvement, the bilateral SNHL associated with isolated cases was mild to profound. There appeared to be some benefit to cochlear implants among individuals who received this intervention.

SPATA5L1 belongs to the AAA+ ATPases protein superfamily, a functionally diverse group of enzymes that hydrolyze ATP to induce changes in target substrates. Variants identified in our cohort are spread throughout the gene and protein (Figure 3A, visualized with Geneious Prime 2021.0.1). Structural effects of a subset of missense variants detected in our cohort were assessed by VIPUR[11] and Missense3D[12] based on a three-dimensional model of SPATA5L1. Of the 13 variants investigated, 11 variants were predicted to have a deleterious effect on protein structure (Figure 3B) via a combination of destabilizing effects, including steric clashes, loss of hydrophobic packing, loss of polar interactions, and the emergence of buried charged residues (Figure S3). All variants predicted to be deleterious are expected to destabilize domains within SPATA5L1, except for the p.Gly689Val variant, which is predicted to create steric clashes with the ATP ligand, affecting ATP-binding properties.

We next sought to define the typical protein localization of SPATA5L1. *SPATA5L1* mRNA has been detected (albeit at low levels) in both neurons and glia, both during embryonic and adult stages of human brain development (Figure 4A). We confirmed this at the protein level in rat dissociated hippocampal cultures, identifying Spata5l1 immunoreactivity within neurons, astrocytes, oligodendrocytes, and microglia; the most prominent staining was in neurons (Figure 4B). *Spata5l1* localized primarily to the nucleus. Within the ear, both inner and outer hair cells exhibit detectable levels of *Spata5l1* transcript (Figure 4C). Rat whole mounts stained with a commercial antibody against Spata5l1 demonstrated that Spata5l1 is present in hair cells and pillar cells of the organ of Corti (Figure 4D), suggesting that loss of wild-type protein may lead to sensorineural hearing loss by disrupting normal function within these structures.

The precise function of SPATA5L1 in brain, inner ear, and other tissues is currently unknown. However, the sequence similarity and overlapping clinical manifestations in individuals harboring putatively loss-of-function or protein-damaging variants in SPATA5 and SPATA5L1 led us to speculate as to a potential redundancy between the two proteins. Given the proposed role of SPATA5 in mitochondrial function,[1] we assessed oxidative phosphorylation (OXPHOS) in primary fibroblasts from affected individuals 2-3, 2-4, 7-9 (i.e., individuals 3 and 4 from family

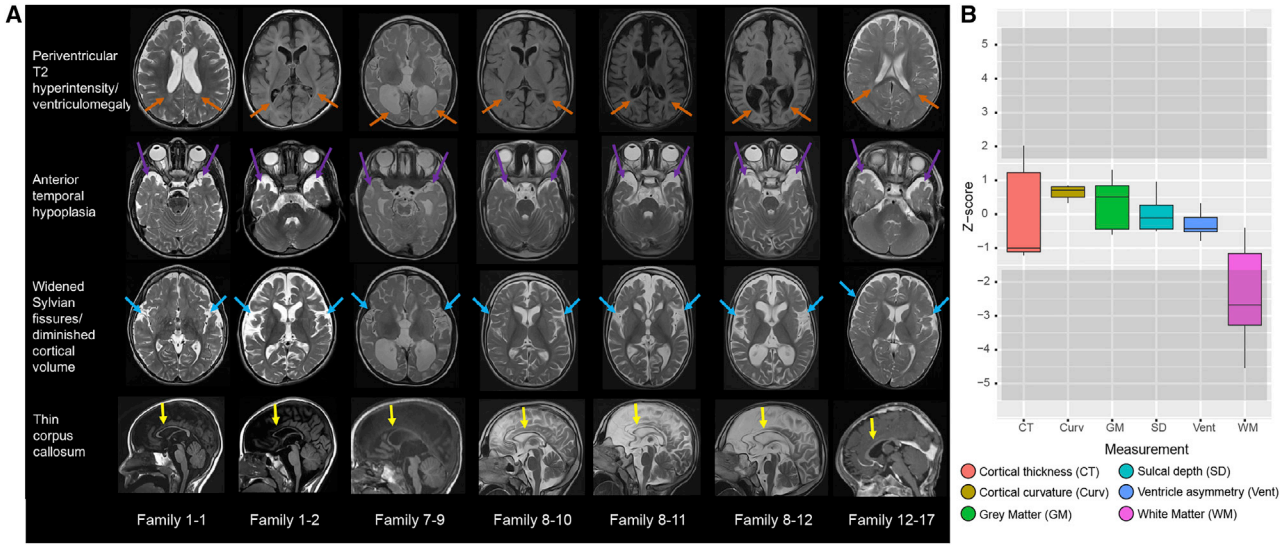

Figure 2. Neuroimaging features in individuals harboring bi-allelic predicted-deleterious variants in *SPATA5L1*

(A) T1 and T2/FLAIR MRI images were assessed for the presence of periventricular leukomalacia (defined as T2 hyperintensity and/or diminished white matter volume/ex vacuo ventriculomegaly evident adjacent to the ventricles); anterior temporal lobe hypoplasia; widened Sylvian fissures (characterized as diminished coverage of the insular cortex), diminished cortical volume; and thin/dysplastic corpus callosum. Ages were 4 years old (1-1, 1-2), 21 years old (7-9), 10 years old (8-10), 7 years old (8-11), 6 years old (8-12), and 1 year old (12-16).

(B) Boxplot of six structural measures quantified from brain MRI volumes, represented as *Z* scores, in comparison to an age-matched control cohort of typically developing children.

2 and individual 9 from family 7) in comparison to passage and age-matched controls by using the Seahorse XF96 assay. These assays indicated no impairment of OXPHOS in affected fibroblasts (Figure S4), suggesting that despite the degree of clinical overlap seen in affected individuals, the two proteins may have divergent functions. Indeed, a mitochondrial localization for SPATA5L1 is not predicted via MitoMiner[13] and it is absent from the MitoCarta3.0 human and mouse inventory.[14] However, alterations to mitochondrial biogenesis remain possible, and we cannot exclude disruption to mitochondrial morphology and dynamics (as observed in SPATA5-deficient neurons).[3]

Next, we turned to an unbiased transcriptome approach to try to distinguish SPATA5L1 fibroblast cell lines from controls. The analysis was performed in the same affected (plus 1-1 and 4-6, i.e., individual 1 from family 1 and individual 6 from family 4) cell lines utilized for the Seahorse study and in passage and age-matched controls. Principal-component analysis from RNA sequencing (RNA-seq) data indicated that individuals harboring bi-allelic SPATA5L1 variants could be distinguished from controls on the basis of their differentially expressed genes (Figure 5A). This provided proof of principle data supporting the p.Ala41Pro, p.Val245Glu, p.Ile435fs, p.Ile466Met, and p.Ala519Asn variants as bona fide disease-associated variants. These findings allowed us to pool these data for subsequent analyses. Significantly upregulated networks were not identified. However, several significantly downregulated genes were identified (Figures 5B and 5C). These genes converged on several hubs (Figures 5D–5F), pointing to a role for SPATA5L1 in mitosis (mitotic nuclear division, sister chromatid segregation, mitotic spindle organization, kinetochores) and DNA replication (DNA conformation change, single-stranded DNA binding, DNA helicase activity). Adhesion receptors, which connect cell-substrate junctions (Figure 5E) and include fibronectin-binding (Figure 5F) integrins (i.e., *ITGA8*; Figure 5B), cadherins (Figure 5F), and immunoglobulin superfamily members (i.e., *L1CAM*; Figure 5B), were significantly downregulated. Members of the AAA+ ATPases protein superfamily have known roles in mitosis, DNA replication, metabolism, and repair processes.[15] For example, cytoplasmic dynein plays a role in mammalian mitotic spindle formation,[16] while WRNIP1 protects stalled replication forks from degradation.[17] Our transcriptome analyses posit a potential role for SPATA5L1 in mitosis and DNA replication, however additional studies are required for assessment of this possibility.

Our clinical, radiologic, genomic, and transcriptomic evidence support the existence of a mixed neurodevelopmental syndrome with hearing loss due to bi-allelic variants in *SPATA5L1*. The pathogenicity of the variants we identified is supported by their rarity (many private variants), predicted deleteriousness by multiple algorithms, consistent phenotype in affected individuals, and RNA-seq validation of several variants. Although we did identify individual loss-of-function (premature stop, frameshift, start-loss, stop-loss, or canonical splice site) alleles, we did not identify bi-allelic loss-of-function variants, suggesting that perhaps human knockout genotypes might show reduced viability. We were not able to clearly identify any firm genotype-phenotype correlations. Our morphologic neuroimaging analyses revealed thin corpus callosum,

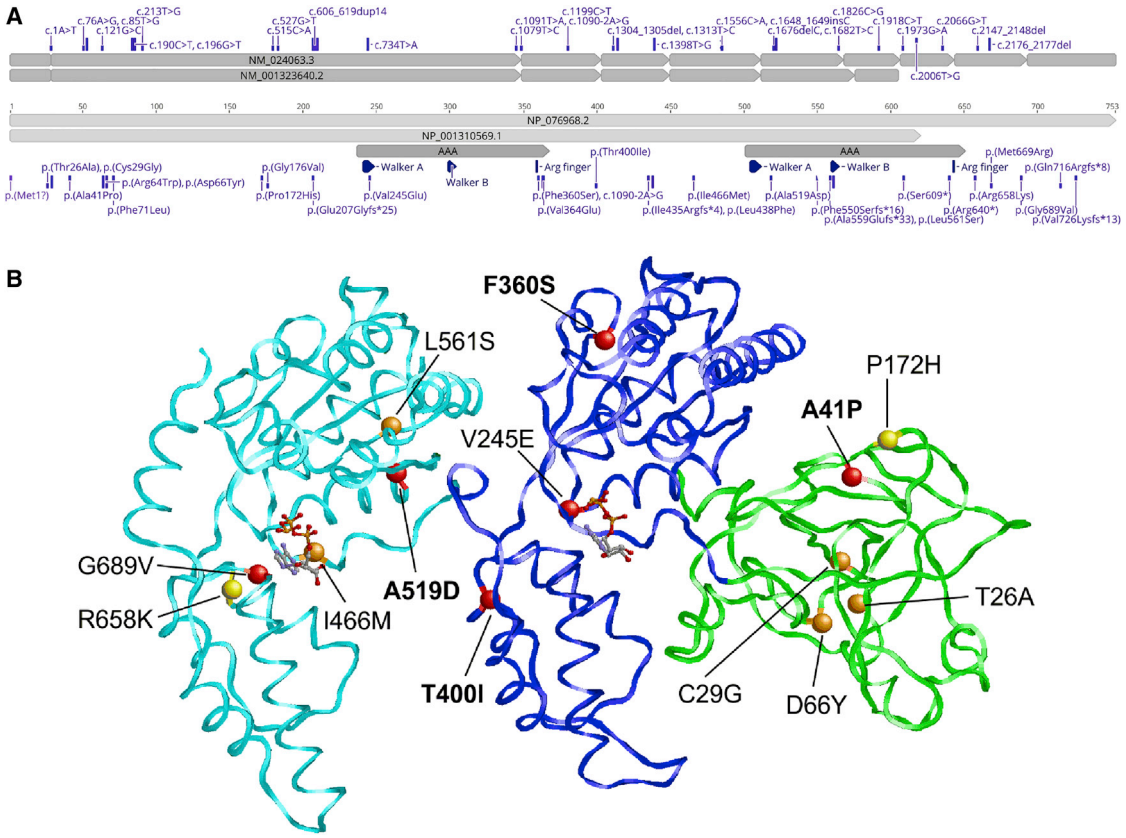

Figure 3. Distribution and predicted structural effects of *SPATA5L1* variants

(A) Alternative splicing leads to two distinct *SPATA5L1* transcripts (top), resulting in a full-length and short isoform (bottom). The variant numbering is based on the full-length transcript and isoform, GenBank: NM_024063.3 and GenBank: NP_076968.2. Non-coding and coding regions of exons are denoted by flat-edged and pointed-edged rectangles, respectively.

(B) Structural effects of a subset of variants identified in this study were evaluated with a three-dimensional model of SPATA5L1 based on the structure of the homologous ATPase p97 (PDB: 5FTN). The SPATA5L1 structure is shown in ribbon presentation, depicting the N-terminal domain (green) and two conserved ATPase domains (AAA, blue and cyan). ATP ligands are shown in stick presentation. Altered residues are highlighted as balls and labeled. Red and orange balls indicate variants that were classified as deleterious by two or one methods, respectively. Yellow balls indicate variants that were predicted to have little effect on protein structure. The variants depicted in more detail in Figure S3 are labeled in bold letters.

diminished cortical volume, open opercula, and anterior temporal hypoplasia in several individuals, while quantitative morphometry indicated that white matter volume was significantly diminished in multiple members of the cohort. When observed, microcephaly correlated with reduced white matter volume (as observed in affected individuals 10-2, 12-1, 13-1).

Although *SPATA5L1* is an orphan gene, our transcriptomic studies provide some clues as to its function. Adhesion receptors collectively play a major role in the control of cell-extracellular matrix (fibronectin-integrin and immunoglobulin superfamily members) and cell-cell interactions (cadherin family members). These interactions in turn integrate cell growth/migration and proliferation on the basis of environmental cues such as contact inhibition. Fibronectin-integrin binding is known to be mediated through focal adhesions, intracellular cytoskeleton/signaling hubs that transmit extracellular cues through phosphorylation events (i.e., protein serine-threonine kinase activator activity) and ultimately control DNA replication and mitosis. Although neuroimaging in our affected individuals did not indicate malformations of cortical development that would suggest abnormalities of neuronal migration, the diminished cortical volumes and microcephaly seen may reflect impairment of neuronal cell division during brain development.

In conclusion, we present evidence that rare coding variants and loss-of-function alleles in *SPATA5L1* lead to hearing loss and a mixed neurodevelopmental disorder that features microcephaly, global developmental delay/intellectual disability, spastic-dystonic cerebral palsy (some children presented with hypotonia), and focal or generalized epilepsy. Although our studies support a role for SPATA5L1 in DNA replication, further experimental studies will be required to support or refute this hypothesis.

Data and code availability

Variants identified in this study have been submitted to ClinVar (accession numbers pending). Original data are available from the authors upon reasonable request.

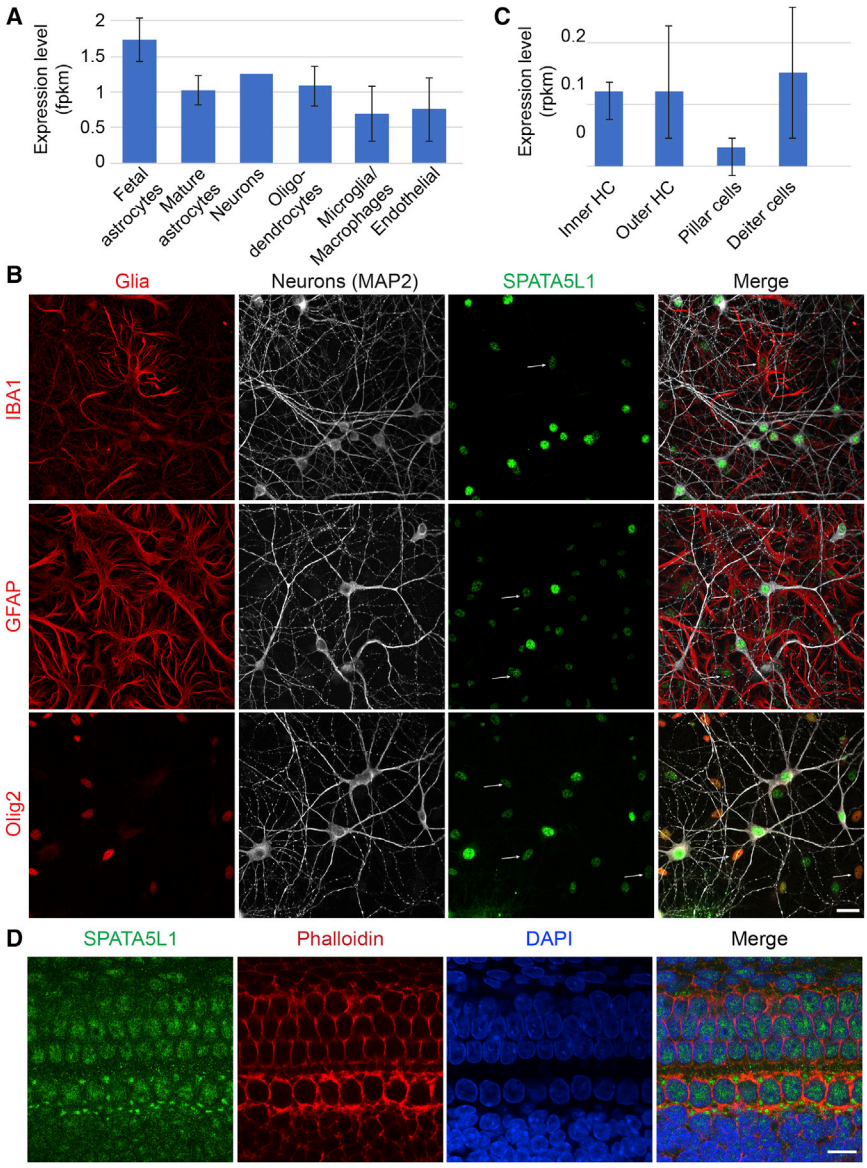

Figure 4. *Spata5l1* is expressed in the inner ear and the brain of rodents/humans

(A) *SPATA5L1* is expressed in all cellular subtypes of the human brain (Brain RNA-Seq database).

(B) Representative immunofluorescent labeling of endogenous SPATA5L1 (green) in rat hippocampal neurons in culture highlight the co-localization of the protein within the nuclei of neurons (MAP2), as well as the nuclei of glial cells (red): microglia (IBA1), astrocytes (GFAP), and oligodendrocytes (Olig2). Signal intensity of SPATA5L1 immunolabeling suggests protein expression is higher in neurons compared to glial cells. Arrows indicate the localization of SPATA5L1 in the nuclei of glial cells. All images are projections of confocal optical section stacks. Scale bar: 25 μm.

(C) *Spata5l1* is expressed at low levels in hair cells (inner and outer) as well as supporting cells (pillar and Deiter cells) in adult mice (adapted from gEAR portal). HC, hair cells.

(D) Representative immunofluorescent labeling of endogenous SPATA5L1 (green) in Sprague Dawley rat organ of Corti at E20. Immunolabeling shows SPATA5L1 is present in the hair and pillar cells of the organ of Corti. DAPI (blue) and Rhodamine Phalloidin (red) were used for counterstaining the nuclei and the cytoskeleton, respectively. All images are projections of confocal optical section stacks. Scale bar: 10 μm.

Supplemental information

Supplemental information can be found online at https://doi.org/10.1016/j.ajhg.2021.08.003.

Acknowledgments

The authors are grateful to the participants and their families, without whose support this work would not have been possible. K.Mc., A.B., A.C., M.J.G.S., R.E.P., and R.E.S. are employees of GeneDx. We thank Minerva Contreras and Thomas Blanpied for assisting with neuronal culture and the CIBR platform (UMSOM, Baltimore, MD, USA). This work was supported in part by R01NS107428 (S.R.), 1R01NS106298 (M.C.K.), and Cerebral Palsy Alliance Research Foundation PG07217 award to W.M. and M.C.K. Portions of this work were also funded by the Fondazione Bambino Gesù (Vite Coraggiose), the Italian Ministry of Health (Ricerca 5 × 1000) to M.T.A., and in part by Telethon Undiagnosed Diseases Program (TUDP, GSP15001). H.L. receives support from the Canadian Institutes of Health Research (Foundation Grant FDN-167281), the Canadian Institutes of Health Research and Muscular Dystrophy Canada (Network Catalyst Grant for NMD4C), the Canada Foundation for Innovation (CFI-JELF 38412), and the Canada Research Chairs Program (Canada Research Chair in Neuromuscular Genomics and Health, 950-232279). B.V. is funded by intramural funding (fortüne) at the University of Tübingen (2545-1-0) and the Ministry of Science, Research, and Art Baden-Württemberg. R.H. is supported by NEI intramural funds. W.K.C. receives support from the JPB Foundation and SFARI. S.C.J. is supported by a K99/R00 Pathway to Independence Award (K99HL143036 and R00HL143036-02) and the Clinical and Translational Research Funding Program award (CTSA1405). This project was funded in part by The Foundation for Barnes-Jewish Hospital and their generous donors and by the NIH/National Center for Advancing Translational Sciences grant UL1TR002345. Several families were enrolled as part of the SYNaPS Study Group collaboration funded by The Wellcome Trust and strategic award (Synaptopathies) funding (WT093205 MA and WT104033AIA). This research was conducted as part of the Queen Square Genomics group at University College London, supported by the National Institute for Health Research University College London Hospitals Biomedical Research Centre. A.P.L.M. was supported by a NHMRC Early Career Research Fellowship (GNT1156820). S.B.'s contributions were funded by a Cerebral Palsy Alliance Research Foundation Career

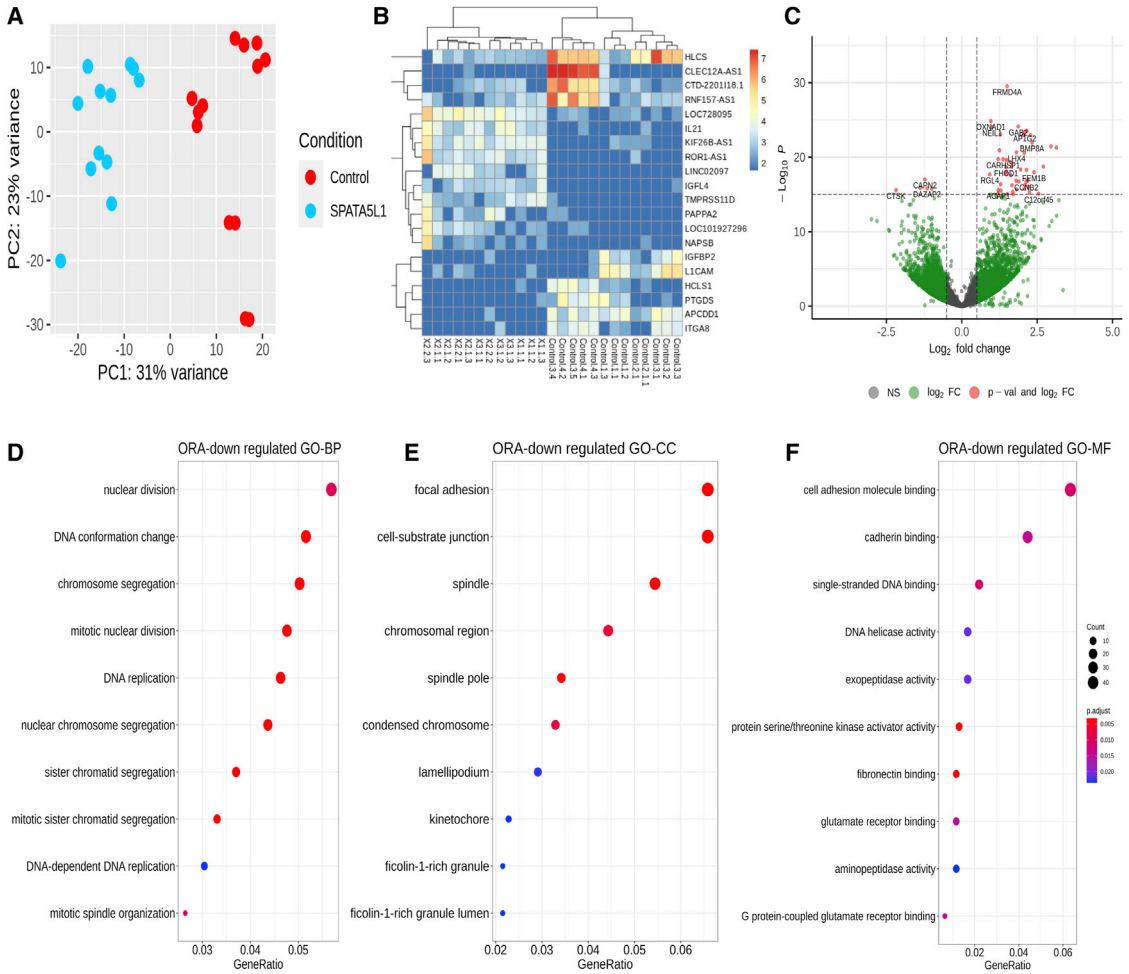

Figure 5. Analysis of gene expression patterns in *SPATA5L1* fibroblasts by RNA-seq reveals differential expression of DNA replication and mitosis-related genes

(A) Principal-component analysis plot shows a differential clustering of SPATA5L1 samples (n = 4) from control samples (n = 4).

(B) Transcriptomic heatmap of the top 20 differentially expressed genes (top ten with fold change > 1.5 and $p < 0.05$ and bottom 10 with fold change < 0.5 and $p < 0.05$). Red/yellow colors represent highly expressed genes and blue colors represent under-expressed genes for these 20 genes in the respective case and control samples. The legend corresponds to expression values.

(C) Volcano plot highlighting genes with large fold changes that are either significantly upregulated or downregulated between SPATA5L1 and control samples. Log_2 fold change of normalized counts (red dots indicate genes with $p < 10^{-16}$).

(D) Over-representation analysis (ORA) for downregulated genes (log_2 fold change < -1, $p < 0.05$) for GO-BP (Gene Ontology Biological Processes).

(E) Over-representation analysis (ORA) for downregulated genes (log_2 fold change < -1, $p < 0.05$) for GO-CC (Gene Ontology Cellular Components).

(F) Over-representation analysis (ORA) for downregulated genes (log_2 fold change < -1, $p < 0.05$) for GO-CC and GO-MF (Gene Ontology Molecular Functions).

Development Award. C.v.E., M.A.C., and A.H.M. were supported by Australian National Health and Medical Research Council Project Grant (1099163). J.G. was supported by Australian National Health and Medical Research Council Fellowship (1041920) and Channel 7 CRF Chair for the Prevention of Childhood Disability. C.v.E. was supported by The Hospital Research Foundation Mid-Career Fellowship. C.v.E., M.A.C., A.H.M., and J.G. were supported by infrastructure funding from the Tenix Foundation. The content is solely the responsibility of the authors and does not necessarily represent the official views of the National Institutes of Health.

Declaration of interests

The authors declare no competing interests.

Received: May 28, 2021
Accepted: August 4, 2021
Published: October 7, 2021

Web resources

Brain RNA-Seq, http://www.brainrnaseq.org/
BrainSpan Atlas of the Developing Human Brain, https://www.brainspan.org/
CADD, https://cadd.gs.washington.edu/
DIOPT, https://www.flyrnai.org/cgi-bin/DRSC_prot_align.pl
gEAR portal, https://umgear.org/
gnomAD, https://gnomad.broadinstitute.org/
MARRVEL, http://marrvel.org/

MutationTaster, http://mutationtaster.org/
OMIM, https://omim.org/
PolyPhen-2, http://genetics.bwh.harvard.edu/pph2/
Provean, http://provean.jcvi.org
SIFT, https://sift.bii.a-star.edu.sg/

References

1. Tanaka, A.J., Cho, M.T., Millan, F., Juusola, J., Retterer, K., Joshi, C., Niyazov, D., Garnica, A., Gratz, E., Deardorff, M., et al. (2015). Mutations in SPATA5 Are Associated with Microcephaly, Intellectual Disability, Seizures, and Hearing Loss. Am. J. Hum. Genet. *97*, 457–464.
2. Liu, Y., Black, J., Kisiel, N., and Kulesz-Martin, M.F. (2000). SPAF, a new AAA-protein specific to early spermatogenesis and malignant conversion. Oncogene *19*, 1579–1588.
3. Puusepp, S., Kovacs-Nagy, R., Alhaddad, B., Braunisch, M., Hoffmann, G.F., Kotzaeridou, U., Lichvarova, L., Liiv, M., Makowski, C., Mandel, M., et al. (2018). Compound heterozygous SPATA5 variants in four families and functional studies of SPATA5 deficiency. Eur. J. Hum. Genet. *26*, 407–419.
4. Köttgen, A., Glazer, N.L., Dehghan, A., Hwang, S.J., Katz, R., Li, M., Yang, Q., Gudnason, V., Launer, L.J., Harris, T.B., et al. (2009). Multiple loci associated with indices of renal function and chronic kidney disease. Nat. Genet. *41*, 712–717.
5. Kubo, Y., Imaizumi, T., Ando, M., Nakatochi, M., Yasuda, Y., Honda, H., Kuwatsuka, Y., Kato, S., Kikuchi, K., Kondo, T., et al. (2017). Association between kidney function and genetic polymorphisms in atherosclerotic and chronic kidney diseases: A cross-sectional study in Japanese male workers. PLoS ONE *12*, e0185476.
6. Park, H., Kim, H.J., Lee, S., Yoo, Y.J., Ju, Y.S., Lee, J.E., Cho, S.I., Sung, J., Kim, J.I., and Seo, J.S. (2013). A family-based association study after genome-wide linkage analysis identified two genetic loci for renal function in a Mongolian population. Kidney Int. *83*, 285–292.
7. Sobreira, N., Schiettecatte, F., Valle, D., and Hamosh, A. (2015). GeneMatcher: a matching tool for connecting investigators with an interest in the same gene. Hum. Mutat. *36*, 928–930.
8. McKenna, A., Hanna, M., Banks, E., Sivachenko, A., Cibulskis, K., Kernytsky, A., Garimella, K., Altshuler, D., Gabriel, S., Daly, M., and DePristo, M.A. (2010). The Genome Analysis Toolkit: a MapReduce framework for analyzing next-generation DNA sequencing data. Genome Res. *20*, 1297–1303.
9. Van der Auwera, G.A., Carneiro, M.O., Hartl, C., Poplin, R., Del Angel, G., Levy-Moonshine, A., Jordan, T., Shakir, K., Roazen, D., Thibault, J., et al. (2013). From FastQ data to high confidence variant calls: the Genome Analysis Toolkit best practices pipeline. Curr. Protoc. Bioinformatics *43*, 11.10.1–11.10.33.
10. Pagnozzi, A.M., Dowson, N., Doecke, J., Fiori, S., Bradley, A.P., Boyd, R.N., and Rose, S. (2017). Identifying relevant biomarkers of brain injury from structural MRI: Validation using automated approaches in children with unilateral cerebral palsy. PLoS ONE *12*, e0181605.
11. Baugh, E.H., Simmons-Edler, R., Müller, C.L., Alford, R.F., Volfovsky, N., Lash, A.E., and Bonneau, R. (2016). Robust classification of protein variation using structural modelling and large-scale data integration. Nucleic Acids Res. *44*, 2501–2513.
12. Ittisoponpisan, S., Islam, S.A., Khanna, T., Alhuzimi, E., David, A., and Sternberg, M.J.E. (2019). Can Predicted Protein 3D Structures Provide Reliable Insights into whether Missense Variants Are Disease Associated? J. Mol. Biol. *431*, 2197–2212.
13. Smith, A.C., and Robinson, A.J. (2016). MitoMiner v3.1, an update on the mitochondrial proteomics database. Nucleic Acids Res. *44* (D1), D1258–D1261.
14. Rath, S., Sharma, R., Gupta, R., Ast, T., Chan, C., Durham, T.J., Goodman, R.P., Grabarek, Z., Haas, M.E., Hung, W.H.W., et al. (2021). MitoCarta3.0: an updated mitochondrial proteome now with sub-organelle localization and pathway annotations. Nucleic Acids Res. *48*, D1541–D1547.
15. Snider, J., Thibault, G., and Houry, W.A. (2008). The AAA+ superfamily of functionally diverse proteins. Genome Biol. *9*, 216.
16. Vaisberg, E.A., Koonce, M.P., and McIntosh, J.R. (1993). Cytoplasmic dynein plays a role in mammalian mitotic spindle formation. J. Cell Biol. *123*, 849–858.
17. Leuzzi, G., Marabitti, V., Pichierri, P., and Franchitto, A. (2016). WRNIP1 protects stalled forks from degradation and promotes fork restart after replication stress. EMBO J. *35*, 1437–1451.